Biosensors and Bioelectronics 143 (2019) 111616

Contents lists available at ScienceDirect

Biosensors and Bioelectronics

journal homepage: www.elsevier.com/locate/bios

A multiple signal amplification sandwich-type SERS biosensor for femtomolar detection of miRNA

Huili Shao[a,1], Han Lin[a,b,1], Zhiyong Guo[a,*], Jing Lu[a], Yaru Jia[a,b], Meng Ye[c,**], Fengmei Su[d], Lingmei Niu[e], Weijun Kang[e], Sui Wang[a], Yufang Hu[a], Youju Huang[b,***]

[a] State Key Laboratory for Quality and Safety of Agro-products, School of Material Science and Chemical Engineering, Ningbo University, Ningbo, 315211, PR China
[b] Key Laboratory of Marine Materials and Related Technologies, Zhejiang Key Laboratory of Marine Materials and Protective Technologies, Division of Polymer and Composite Materials, Ningbo Institute of Materials Technology & Engineering, Chinese Academy of Sciences, Ningbo, 315201, PR China
[c] Department of Medical Oncology, The Affiliated Hospital of Medical School, Ningbo University, Ningbo, 315020, PR China
[d] National Engineering Research Centre for Advanced Polymer Processing Technology, Key Laboratory of Materials Processing and Mold (Zhengzhou University), Ministry of Education, Zhengzhou University, Zhengzhou, 450002, PR China
[e] School of Public Health, Hebei Medical University, Shijiazhuang, 050017, PR China

ARTICLE INFO

Keywords:
SERS biosensors
miRNA
Gold nanowire vesicles
Hybridization chain reaction
Silver stain
Multiple signal amplification

ABSTRACT

MicroRNAs are widely used as tumor markers for cancer diagnosis and prognosis. Herein, a multiple signal amplification sandwich-type SERS biosensor for femtomolar detection of miRNA is reported. The signal unit consisted of giant Au vesicles, DNA sequences and deposited silver nanoparticles. The giant Au vesicles provided large-volume hot spots because of sharp tips and abundant hotspot gaps, thus enhancing the electromagnetic intensity for the SERS performance. Further silver stain would easily lead to second-stage amplification of Raman signal. In addition, more SERS signal molecules R6G adsorbed on the signal unit with the aid of HCR and the controlled nanogaps between adjacent AgNPs, brought about the third-stage amplification. The capture unit, prepared by immobilizing the capture probe (CP) on the Fe_3O_4@AuNPs, could easily capture target miRNA and greatly simplify the separation step to improve reproducibility. The higher concentration of target miRNA definitely formed more sandwich-type structures with combination of capture unit and signal unit, resulting in multiple amplification of SERS signals. The proposed multiple signal amplification sandwich-type SERS biosensor could detect miRNA-141 at the femtomolar level with a low detection limit of 0.03 fM. Meanwhile, it exhibited high selectivity and accuracy, even for practical analysis in human serum. Therefore, the designed multiple signal amplification sandwich-type SERS biosensor would be a very promising alternative tool for the detection of miRNA and analogs in the field of biomedical diagnosis.

1. Introduction

Cancer has been considered as one of the most dangerous health threats and the leading cause of death worldwide (Robison and Hudson, 2014; Wulfkuhle et al., 2003). Screening tests can find not only early cancers but also abnormal precancerous cells that have a high chance of turning into cancers. It is thus greatly in favor of cancer prevention and timely treatment. However, hidden aetiological causes and no clinical symptoms are typical in cancer onset (Maruthappu et al., 2016; Schwarzenbach et al., 2011), severely restricting effective screening of cancers in the early stage. In recent high-profile studies, the distinct levels of miRNAs, particularly circulating miRNAs in serum, have demonstrated a promising application potential to become new biomarkers for cancer diagnosis and prognosis (Gai et al., 2018; Hou et al., 2015; Lin and Gregory, 2015; Lu et al., 2005). For example, miRNA-141, an endogenous non-coding RNA containing 22 nucleotides, has been verified as an important tumor marker for detecting the breast and prostate cancer cells (Jou et al., 2015; Li et al., 2017). Currently, a large number of efforts have achieved successes in the detection of miRNA, including quantitative reverse-transcriptase polymerase chain reaction (qRT-PCR) (Redshaw et al., 2013), microarrays (Lagos-Quintana et al., 2001), and Northern blotting (Thomson et al., 2004), etc. However,

* Corresponding author.
** Corresponding author.
*** Corresponding author.
E-mail addresses: guozhiyong@nbu.edu.cn (Z. Guo), yemeng@nbu.edu.cn (M. Ye), yjhuang@nimte.ac.cn (Y. Huang).
[1] Those authors contributed equally to this work.

https://doi.org/10.1016/j.bios.2019.111616
Received 27 June 2019; Received in revised form 7 August 2019; Accepted 19 August 2019
Available online 22 August 2019
0956-5663/

these strategies suffer from the low abundance of miRNA in total RNA samples (femtomolar level in concentration) and the susceptibility to degradation, resulting in unexpected deficiencies in the actual detection. For instance, large volume of sample and designing primers are required. It is easy to cause cross-hybridization and the overall operation procedures are too complicated. In this regard, it is in great demand to develop an accurate, sensitive and easy method for detecting miRNA.

Surface enhancement Raman scattering (SERS) technology possesses a good deal of superiorities like high sensitivity, narrow spectral band (Guo et al., 2015; Li et al., 2015b) and abundant fingerprint information (Zhang et al., 2013), bringing a series of advantages for the detection of miRNA. First, it is able to facilitate the molecular-level identification of samples. Second, the sample preparation and operation are very easy and nondestructive, which is suitable for the detection of a wide variety of matrices (Chen et al., 2016; Guarrotxena and Bazan, 2014; Huang et al. 2015, 2016; Lu et al., 2018; Rong et al., 2017). Therefore, it has been widely used to detect biomolecules at trace level, such as nucleic acids (Zeng et al., 2014), proteins (Ye et al., 2014b), small molecules (Zhang et al., 2013) and so on. To achieve ultra-trace detection of biomolecules, SERS signals should be further enhanced through either preparing efficient substrates or increasing the number of Raman signal molecules (Lane et al., 2015; Wang et al., 2013). Currently, a variety of SERS substrates with different structures of nanomaterials have been prepared for the construction of SERS-active biosensors, such as magnetic Fe_3O_4@Au@Ag (Ding et al., 2016), Ni-Fe@Au (Li et al., 2015a), Au–Ag core-shell structure (Cha et al., 2015; Gunawidjaja et al., 2008), nanohollows (Chon et al., 2009; Lee et al., 2014), aggregates (Wilson and Willets, 2014), etc. Our group prepared a kind of Au nanowire vesicles (AuNWs) as a novel SERS substrate with rich sharp tips, high surface area and good biocompatibility (Guo et al., 2018; Jia et al., 2017). In addition, silver ions could be reduced to silver atoms by hydroquinone under the catalysis of Au wires and thus the surface became rougher, leading to an effective enhancement of SERS signal intensity.

Hybridization chain reaction (HCR) is an enzyme-free amplification technique through which the initiator can trigger the hybridization and result in the polymerization of oligonucleotides into long nicked dsDNA polymers under mild conditions. Aside from the great potential in the direct detection of nucleic acid (Li et al., 2015c; Pang et al., 2016; Zheng et al., 2015), it was also tried to enhance the SERS signal. Because a number of silver ions were absorbed by the electrostatic interaction on the HCR-prolonged DNA skeleton and then reduced to form silver nanoparticles, the SERS signal was amplified by adsorbing lots of SERS reporter molecules on silver nanoparticles (Gao et al., 2013; Qian et al., 2018).

Herein, using miRNA-141 as a research model, a multiple signal amplification sandwich-type SERS biosensor for ultrasensitive detection of femtomolar miRNA was constructed by a combination of AuNWs, silver stain and HCR, with a detection limit of 0.03 fM. In addition, the proposed biosensor could be very simply prepared by only two incubation steps once the capture unit and the signal unit were ready, giving rise to a good reproducibility. This work, therefore, shows a great promise for the miRNA quantification at trace level and may find broad applications in early clinical diagnostics of cancers.

2. Experimental

2.1. Materials

Poly(N-vinylpyrrolidone) (PVP, MW = 550,000), 3-amino-propyltriethoxysilane (APTES), sodium citrate tribasic dihydrate (99.0%), L-ascorbic acid (L-AA), and 4-mercaptobenzoic acid (MBA, 90%) were purchased from Sigma-Aldrich (St. Louis, MO, USA). 2,2-azobisisobutyronitrile (AIBN) was obtained from Aladdin (Shanghai, China), and recrystallized three times from methanol before use. Styrene was purchased from Aladdin (Shanghai, China), and distillated to refine under reduced pressure. Chloroauric acid ($HAuCl_4{\cdot}4H_2O$, 99.9%), hydroquinone, silver nitrate ($AgNO_3$), rhodamine 6G (R6G), 6-mercapto-1-hexanol (MCH) and other chemicals were purchased from Sinopharm Chemical Reagent Co., Ltd. (Shanghai, China), and used as received. Milli-Q water (18.2 MΩ cm) was used for all experiments. All oligonucleotides were synthesized and purified by Sangon Biotechnology Co., Ltd. (Shanghai, China). The sequences of nucleic acids are depicted in Table S1. Buffers involved in this work are shown in the Supporting Information.

2.2. Instruments

Morphologies of different nanomaterials were visualized by the scanning electron microscopy (SEM, Hitachi SU-70, Tokyo, Japan) at an accelerating voltage of 15–20 kV and the transmission electron microscopy (TEM, JEM-2100, Electronic Co., Ltd., Japan) at an accelerating voltage of 200 kV. Raman charts were obtained on an inVia Reflex micro Raman spectrometer (Renisho, UK).

2.3. Synthesis of the capture unit (Fe_3O_4@AuNPs-CP)

The capture probe (CP) was diluted with a DNA hybridization buffer I to 1 μM, heated in a water bath at 95 °C for 5 min, and then slowly cooled to room temperature to form a hairpin structure of the CP chains and activate thiol groups. Then, 100 μL of 1 μM hairpin CP and 200 μL of 1 mg/mL Fe_3O_4@AuNPs solution (Liu et al., 2014) (see the Supporting Information) were mixed and incubated in the dark for 24 h, the hairpin CP was fully combined to the surface of Fe_3O_4@AuNPs through Au–S bonds. Subsequently, 50 μL of 1 mM MCH solution was added to block non-specific adsorption sites. Finally, capture unit Fe_3O_4@AuNPs-CP was obtained after washing and reconstituted in a 100 μL of DNA hybridization buffer II. The capture unit was magnetic and was easily captured on the surface of the magnetic electrode, greatly simplifying the separation step and thus then effectively improving the repeatability and reproducibility.

2.4. Synthesis of the signal unit (AuNWs/HCR@AgNPs@R6G)

Gold nanowire vesicles (AuNWs) were prepared as previously reported. Briefly, Au seed-coated PS microspheres (PS-AuNPs) were prepared by coating gold nanoparticles (AuNPs) on amino-decorated polystyrene (PS) microspheres. Then, AuNWs were constructed via combined “anisotropic growth” and “sacrificing template” strategies based on PS-AuNPs. The detailed procedures could be found in the Supporting Information (Jia et al., 2017; Guo et al., 2018; Nie and Emory, 1997; Kim and Suh, 2008). Firstly, 100 μL of 1 μM the trigger probe (TP) was added into 400 μL of AuNWs. After incubating for 24 h, AuNWs/TP were obtained by Au–S bonds and reconstructed in 200 μL of DNA hybridization buffer II. After that, 20 μL of 1 μM H1 and 20 μL of 1 μM H2 solution were simultaneously added into 200 μL of AuNWs/TP and reacted for 2 h. In the presence of H1 and H2 which is partially complementary to H1, dsDNA was obtained through in situ HCR to produce AuNWs/HCR. Subsequently, 20 μL of 10 mM $AgNO_3$ solution was added into the AuNWs/HCR solution and reacted for 30 min in dark. After washing with DNA hybridization buffer II, 20 μL of 10 g/L hydroquinone solution was added dropwise for 30 min to reduce silver ions to form AuNWs/HCR@AgNPs. After 10 μL of 0.01 M R6G solution was added, incubated for 2 h and washed, the signal unit AuNWs/HCR@AgNPs@R6G was finally obtained.

2.5. Fabrication of the SERS biosensor

A 20 μL of as-prepared capture unit solution and 10 μL of the target miRNA-141 with different concentrations were mixed and incubated at 37 °C for 1.5 h. After washing with DNA hybridization buffer II by

magnetic separation, 20 μL of signal unit solution was added and incubated at 37 °C for 1.5 h, followed by rinsing and reconstituting in 50 μL of DNA hybridization buffer II. Finally, the resulting solution was applied for the SERS signal collection using a confocal Raman microscopy system with the default parameters as follows: He–Ne laser excitation wavelength = 632.8 nm; excitation power = 1.5 mW; 50x telephoto lens (NA = 0.75). Therefore, the fabrication of the SERS biosensor can be completed very simply once the capture unit and the signal unit were ready.

2.6. Process of real sample preparation

Serum of 3 healthy volunteers and 3 prostate cancer patients were collected with informed consent, and detected as soon as possible. A 10 μL of serum sample was applied to detect directly without any pretreatment, and diluted appropriately to meet the established standard curve if needed.

3. Results and discussion

3.1. Preparation procedure and detection principle

The preparation procedure and detection principle of multiple signal amplification sandwich-type SERS biosensor is shown in Scheme 1. It contained two components, *i.e.*, the signal unit and the capture unit. In the formation of the signal unit, TP was first immobilized on the surface of AuNWs via Au–S bonds. Two hairpin DNA sequences of H1 and H2 were subsequently introduced to the AuNWs-TP solution, in situ propagating the hybridization chain reaction to obtain dsDNA in the presence of TP. When $AgNO_3$ solution was added, silver ions were then adsorbed on the AuNWs and intercalated into the skeleton of dsDNA by the electrostatic interaction (Gao et al., 2013; Qian et al., 2018). The silver nanoparticles emerged on the nanostructures of AuNWs and dsDNA to form the AuNWs/HCR@AgNPs after the reduction using hydroquinone. Finally, the Raman signal molecule R6G was adsorbed to form the signal unit on the surface of the silver nanoparticles. The capture unit was prepared by immobilizing hairpin CP on the Fe_3O_4@AuNPs, which could easily capture target miRNA-141 and be attracted onto the surface of the MGCE under a magnetic field. In the presence of target miRNA-141 which could hybridize with CP, the CP stem-loop structure on the capture unit was opened to form a partial dsDNA, making the end residues sequence of CP to couple with H2 which was exposed on the signal unit to achieve a successful immobilization. In this way, the higher the concentration of miRNA-141 definitely produces more signal units combined, resulting in a higher SERS intensity. Therefore, an emerging detection principle is that the concentration of miRNA can be detected by monitoring the change in SERS signal intensities.

3.2. Characterization of the nanomaterials

As depicted in Fig. 1A, PS microspheres prepared by the dispersion polymerization (see the Supporting Information) display a diameter of about 3 μm and a smooth surface. The further amino-modification of the surface using APTES promotes the binding between AuNPs and PS microspheres. Fig. 1B shows that the surface of PS-AuNPs is rough with a large number of distributed AuNPs. In Fig. 1C, AuNWs are tightly deposited on the surface of PS microspheres, followed by dissolving PS with tetrahydrofuran (THF). As shown in Fig. 1D, the gold nanowires of the signal unit are distributed by a large number of AgNPs, resulting in a significant thickening of gold nanowires after silver stain and a smaller morphology with some voids on the surface. It is worth noting that most of signal units can support themselves as a cavity on account of their close packing. The inset image in Fig. 1D shows a slightly broken signal unit, obviously confirming its hollow structure. The elemental compositions of Fe_3O_4@AuNPs were verified by SEM and EDS results (Fig. S1). The morphology of the capture unit prepared by immobilizing CP on the Fe_3O_4@AuNPs is shown in Fig. 1E. It can be seen that Fe_3O_4 nanospheres with a diameter of about 80–100 nm were fully covered by a number of gold nanoparticles with a diameter of about 10–15 nm, which have the capability to bind CP through the Au–S coordination. When miRNA-141 is present, the complex signal unit-

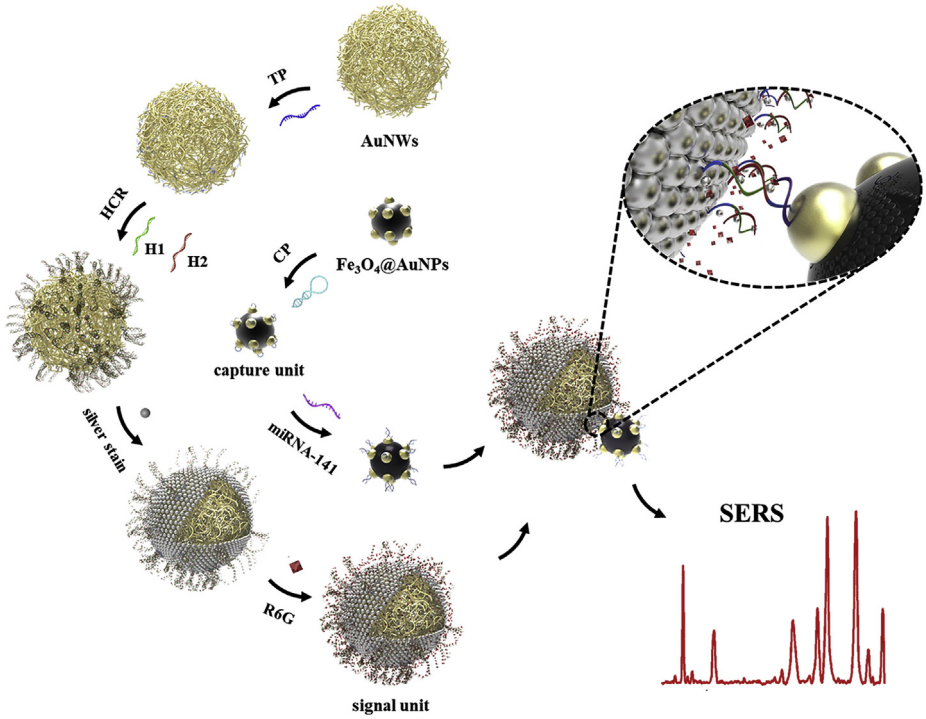

Scheme 1. Schematic diagram of the preparation procedure of the signal unit and the fabrication of the proposed multiple signal amplification sandwich-type SERS biosensor for miRNA detection.

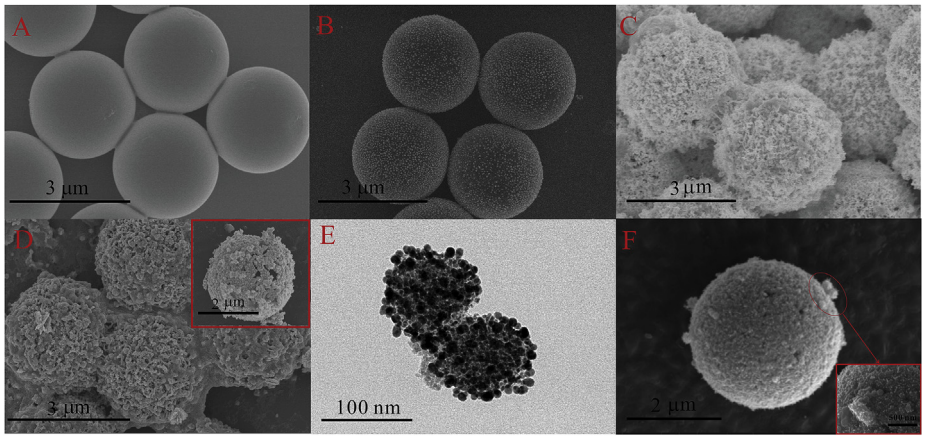

Fig. 1. SEM images of (A) PS microspheres, (B) PS-AuNPs, (C) AuNWs, (D) signal unit (inset: a broken one) and (F) capture unit-miRNA-141-signal unit. TEM image of (E) capture unit.

miRNA141-capture unit is formed very easily and ready for the ultrasensitive SERS detection of femtomolar miRNA-141 based on the proposed multiple amplification strategy (Fig. 1F).

3.3. Mechanism of the multiple signal amplification

R6G, a Raman signal molecule, was used to investigate the SERS performance of the biosensor. The mechanism of the multiple signal amplification was investigated through a series of controlled experiments. As shown in Fig. 2A, when R6G is directly coated on a bare silicon slice, the SERS signal is too weak to be detected (curve a). In the case of AuNWs, several distinctive Raman signals at 612, 774, 1181, 1310, 1361, 1509, 1572, and 1650 cm^{-1} are found in the Raman spectra when R6G is adsorbed (curve b). The SERS signal intensity is obviously strengthened due to the excellent SERS effect of AuNWs. It provides large-volume hot spots and sharp tips to form a tip-to-tip structure and abundant gaps, thus generating the maximum electric field enhancement because of the lightning rod effect and the resulting better SERS performance(Barbosa et al., 2010; Liu et al., 2013). For AuNWs@AgNPs, a large number of silver nanoparticles are loaded onto the AuNWs surface through the reduction of Ag^{+} by hydroquinone. It brings a much rougher surface to induce a higher SERS signal intensity (curve c)(Gao et al., 2013; Guo et al., 2018), receiving a second-stage signal amplification. In the case of AuNWs/HCR@AgNPs, the DNA skeleton which could be extended after HCR are introduced. More silver nanoparticles can thus be deposited to adsorb more SERS signal molecules R6G, and the nanogaps between adjacent AgNPs controlled by DNA chains inherently generate strong coupling and highly reproducible SERS reactivity (Zhang et al., 2017), leading to a third-stage amplification of the SERS signal (curve d). In a word, the SERS signal intensity of the proposed biosensor can be greatly enhanced through the multiple signal amplification. To further demonstrate the mechanism, comparison experiments using AuNPs (curve a), AuNWs (curve b), AuNWs@AgNPs (curve c) and AuNWs/HCR@AgNPs (curve d) based signal unit for the practical detection of 1 pM miRNA-141 were carried out, as shown in Fig. 2B. The SERS signal gradually increased, confirming the multiple signal amplification again.

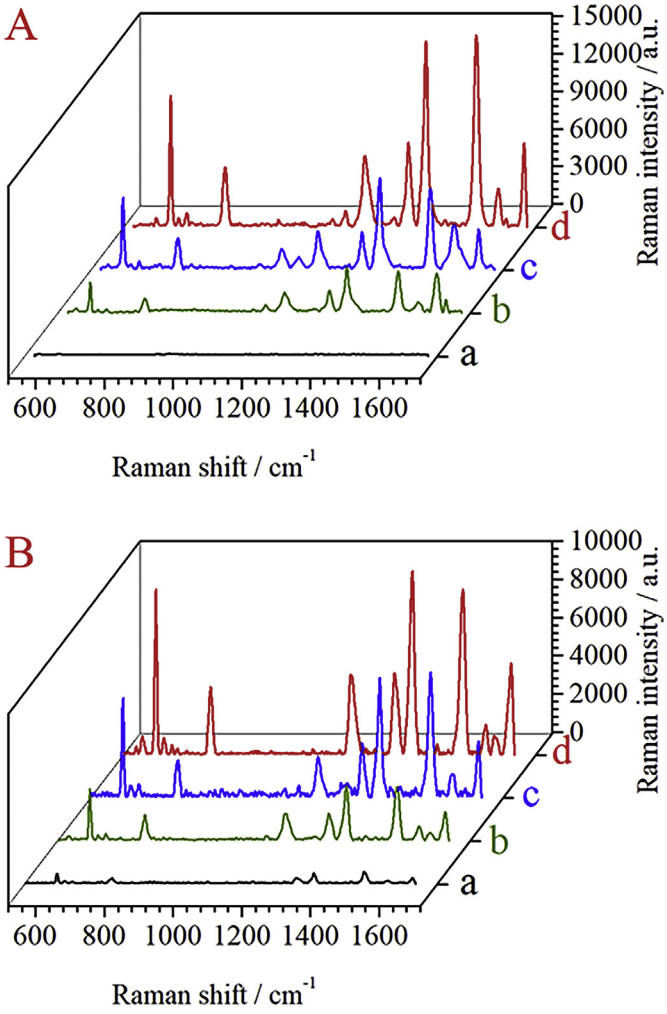

Fig. 2. (A) SERS spectra of R6G acquired from (a) bare silicon coating, (b) AuNWs, (c) AuNWs@AgNPs and (d) AuNWs/HCR@AgNPs. (B) Comparison experiments using AuNPs (curve a), AuNWs (curve b), AuNWs@AgNPs (curve c) and AuNWs/HCR@AgNPs (curve d) based signal unit for the practical detection of 1 pM miRNA-141. (For interpretation of the references to colour in this figure legend, the reader is referred to the Web version of this article.)

3.4. Optimization of the detection conditions

According to the multiple signal amplification discussed above, the signal intensity is strongly related to the number of R6G adsorbed on the surface due to the significant effect of silver stain on the surface roughness as well as the number of Ag nanoparticles. $AgNO_3$ concentration and R6G concentration were therefore optimized in the presence of 100 fM target miRNA-141. As shown in Fig. S2, the maximum Raman intensity can be achieved when 1.0 mM of $AgNO_3$ and 0.5 mM of R6G are used, respectively, which exhibits the optimized detection conditions. Under defined experimental conditions such as

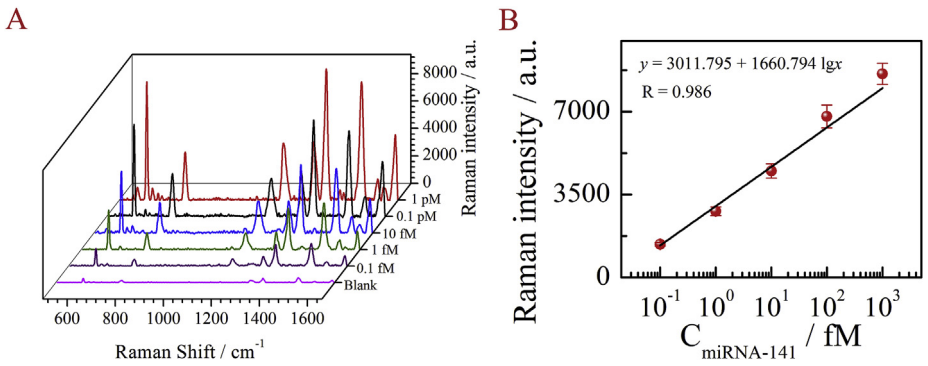

Fig. 3. (A) SERS spectra of R6G for the quantitative evaluation of miRNA-141 with different concentrations; (B) The linear relationship between the Raman intensity and the logarithm of miRNA-141 concentration from 0.1 to 1000 fM.

deposition time, hydroquinone concentration and so on, the increase in silver ions concentration means an increase in the size of the silver nanoparticles, so the SERS signal intensity increases. When the size of the silver nanoparticles increases to a certain extent, more light is scattered through inelastic scattering resulting in a maximum SERS signal intensity (Gao et al., 2013; Stamplecoskie et al., 2011). As to R6G, when its concentration increases, the SERS intensity increases gradually and then trends to a constant value, due to the adsorption amount of R6G which directly affected the SERS signal gradually increases and tends to saturate.

3.5. Linearity and sensitivity

Under the optimized experimental conditions, the performance of the multiple signal amplification sandwich-type SERS biosensor for quantitative analysis of miRNA-141 was further investigated. As shown in Fig. 3A, the Raman signal intensity enhances with increasing the miRNA-141 concentration. A good linear relationship of Raman signal intensity versus logarithm of miRNA-141 concentration in the range of 0.1 fM to 1.0 pM can be found (Fig. 3B). The regression equation can be expressed as $y = 3011.795 + 1660.794 \lg x$ with a correlation coefficient R of 0.986 and a detection limit of 0.03 fM based on the signal noise ratio S/N = 3, where y is the Raman signal intensity and x is the target miRNA-141 concentration. Compared with the previously published reports (Guven et al., 2014; Li et al., 2016; Ma et al., 2018; Su et al., 2017; Ye et al., 2014a; Zhang et al., 2015; Zheng et al., 2015) shown in Table S2, the SERS biosensor shows better performance in the sensitivity due to the designed multiple signal amplification aforementioned.

3.6. Selectivity, stability and reproducibility

To investigate the selectivity of the multiple signal amplification sandwich-type SERS biosensor, different possible interferences were assessed under the same experimental conditions, and the results are summarized in Fig. S3. When the biosensor was respectively incubated with miRNA-21, non-complementary sequence (NC), three-base mismatched target (3 MT), and single-base mismatched target (1 MT) at the concentration of 1 pM, there is no apparent change of the Raman intensity compared to the blank test. However, when 0.1 fM of target miRNA-141 coexisted with those interferences, the Raman signal intensity is almost same as that of only 0.1 fM miRNA-141, indicating a good specificity for the detection miRNA-141 using the proposed biosensor.

Stability is another important factor to estimate the performance of the proposed biosensor. After the capture unit and the signal unit solution were stored in a refrigerator at 4 °C for two weeks, the SERS intensity for the detection of 0.1 fM miRNA-141 was 92.7 ± 6.7% of the initial value (Table S3), which was obtained when the sensor was constructed freshly. This result suggests an acceptable storage stability of the proposed biosensor.

The magnetic capture unit combining with a large number of specific recognition DNA sequence greatly simplifies the capture and separation steps of the target miRNA. Thanks to the very simple preparation procedure of the proposed biosensor, the reproducibility is satisfied, which could be clearly demonstrated by that ten replicate measurements of target miRNA-141 at 1 fM showed relative standard deviation (RSD) of 6.9% (Table S4).

3.7. Application in spiked samples

To further validate the reliability and capability of the proposed SERS biosensor, recoveries were tested by determining spiked miRNA-141 samples with different concentrations which were prepared by adding synthetic miRNA-141 to blank human serum. The human serum was collected from a healthy volunteer, in which miRNA-141 was not found by this proposed method. As shown in Table 1, recoveries were obtained from 93.5 to 110.2% and RSDs were between 5.8 and 9.3%, indicating the potentiality of this SERS biosensor for miRNA-141 detection in clinical applications.

3.8. Application in real samples

Serum samples of 3 healthy volunteers and 3 prostate cancer patients were collected to test the circulating miRNA-141. To facilitate the data comparison, measurement unit fM is conversed to coyies/μL. As shown in Table 2, the amounts of circulating miRNA-141 were found to be highly expressed in prostate cancer samples, and they were within the concentration range of those determined by the single-molecule catalytic hairpin assembly (smCHA) and the "gold standard" method for miRNA detection reverse transcription quantitative PCR (RT-qPCR) (Hu et al., 2018).

4. Conclusions

In summary, a very simple and multiple signal amplification sandwich-type SERS biosensor has been developed for the detection of femtomolar miRNA-141. In this SERS biosensor, (1) the sharp tips and

Table 1
Recovery tests for miRNA-141 in spiked human serum samples ($\bar{x} \pm s$, $n = 5$).

Samples	Added (fM)	Obtained (fM)	RSD (%)	Recovery (%)
serum 1	0.1	0.108 ± 0.010	9.3	108.0
serum 2	1	1.102 ± 0.094	8.5	110.2
serum 3	10	10.50 ± 0.76	7.2	105.0
serum 4	100	93.5 ± 5.4	5.8	93.5
serum 5	1000	957 ± 58	6.1	95.7

Table 2
Quantification of miRNA-141 in human serum from 3 healthy volunteers and 3 prostate cancer patients ($\bar{x} \pm s$, $n = 5$).

Samples	Found by this method (fM)	Equivalent to (copies/μL)
healthy volunteer 1	Not found	–
healthy volunteer 2	7.8 ± 0.6	4699 ± 361
healthy volunteer 3	2.9 ± 0.3	1745 ± 180
prostate cancer patient 1	137 ± 16	82529 ± 9638
prostate cancer patient 2	61.3 ± 5.5	36927 ± 3313
prostate cancer patient 3	426 ± 67	256622 ± 40334

abundant tip-tip gaps of Au vesicles can significantly amplify the SERS signal; (2) silver stain can greatly increase the surface roughness and easily lead to the second-stage enhancement of Raman signal intensity; (3) with the aid of HCR, the DNA skeleton could be extended to deposit more silver nanoparticles for adsorbing more signal molecules R6G, resulting in the third-stage amplification. Benefitting from such sandwich-type SERS structure and the resultant multiple signal amplification, ultra-trace miRNA-141 can be detected with a very low detection limit 0.03 fM. The specificity, stability, reproducibility, precision and application of multiple signal amplification sandwich-type SERS biosensor are also satisfied. In fact, this work builds a technology platform for detecting miRNAs. Only by adjusting the capture unit and the signal unit according to the base sequence of the research object, we can detect various miRNAs and analogs. Therefore, this easy-to-prepare and versatile sandwich-type SERS biosensor with multiple signal amplification has a wide potential application in the clinical diagnosis of cancers.

CRediT authorship contribution statement

Huili Shao: Writing - original draft, Investigation, Data curation, Formal analysis. **Han Lin:** Writing - original draft, Investigation, Visualization. **Zhiyong Guo:** Conceptualization, Methodology, Project administration, Supervision, Writing - review & editing, Funding acquisition. **Jing Lu:** Methodology. **Yaru Jia:** Methodology, Resources. **Meng Ye:** Conceptualization, Resources. **Fengmei Su:** Validation, Software. **Lingmei Niu:** Methodology. **Weijun Kang:** Methodology. **Sui Wang:** Methodology. **Yufang Hu:** Methodology. **Youju Huang:** Conceptualization, Methodology, Project administration, Supervision, Writing - review & editing, Funding acquisition.

Declaration of competing interest

The authors declare that they have no known competing financial interests or personal relationships that could have appeared to influence the work reported in this paper.

Acknowledgments

We gratefully acknowledge the National Natural Science Foundation of China (41576098, 81773483, 51873222, 21605089), the Fujian Province-Chinese Academy of Sciences STS project (2017T31010024), the Youth Innovation Promotion Association of the Chinese Academy of Science (2016268) and the Science and Technology Department of Zhejiang Province of China (2016C33176). This work was also sponsored by K.C. Wong Magna Fund at Ningbo University.

Appendix A. Supplementary data

Supplementary data to this article can be found online at https://doi.org/10.1016/j.bios.2019.111616.

References

Barbosa, S., Agrawal, A., Rodriguez-Lorenzo, L., Pastoriza-Santos, I., Alvarez-Puebla, R.A., Kornowski, A., Weller, H., Liz-Marzan, L.M., 2010. Tuning size and sensing properties in colloidal gold nanostars. Langmuir 26 (18), 14943–14950.
Cha, S.K., Mun, J.H., Chang, T., Kim, S.Y., Kim, J.Y., Jin, H.M., Lee, J.Y., Shin, J., Kim, W.H., Kim, S.O., 2015. Au/Ag core/shell nanoparticle array by block copolymer lithography for synergistic broadband plasmonic properties. ACS Nano 9, 5536–5543.
Chen, J., Huang, Y., Kannan, P., Zhang, L., Lin, Z., Zhang, J., Chen, T., Guo, L., 2016. Flexible and adhesive surface enhance Raman scattering active tape for rapid detection of pesticide residues in fruits and vegetables. Anal. Chem. 88 (4), 2149–2155.
Chon, H., Lee, S., Son, S.K., Oh, C.H., Choo, J., 2009. Highly sensitive immunoassay of lung cancer marker carcinoembryonic antigen using surface-enhanced Raman scattering of hollow gold nanospheres. Anal. Chem. 81, 3029–3034.
Ding, Q., Zhou, H., Zhang, H., Zhang, Y., Wang, G., Zhao, H., 2016. 3D Fe_3O_4@Au@Ag nanoflowers assembled magnetoplasmonic chains for in situ SERS monitoring of plasmon-assisted catalytic reactions. J. Mater. Chem. 4 (22), 8866–8874.
Gai, P., Gu, C., Hou, T., Li, F., 2018. Integration of biofuel cell-based self-powered biosensing and homogeneous electrochemical strategy for ultrasensitive and easy-to-use bioassays of microRNA. ACS Appl. Mater. Interfaces 10 (11), 9325–9331.
Gao, F., Lei, J., Ju, H., 2013. Label-free surface-enhanced Raman spectroscopy for sensitive DNA detection by DNA-mediated silver nanoparticle growth. Anal. Chem. 85 (24), 11788–11793.
Guarrotxena, N., Bazan, G.C., 2014. Antitags: SERS-encoded nanoparticle assemblies that enable single-spot multiplex protein detection. Adv. Mater. 26 (12), 1941–1946.
Gunawidjaja, R., Peleshanko, S., Ko, H., Tsukruk, V.V., 2008. Bimetallic nanocobs: decorating silver nanowires with gold nanoparticles. Adv. Mater. 20 (8), 1544–1549.
Guo, P., Sikdar, D., Huang, X., Si, K.J., Xiong, W., Gong, S., Yap, L.W., Premaratne, M., Cheng, W., 2015. Plasmonic core-shell nanoparticles for SERS detection of the pesticide thiram: size- and shape-dependent Raman enhancement. Nanoscale 7 (7), 2862–2868.
Guo, Z., Jia, Y., Song, X., Lu, J., Lu, X., Liu, B., Han, J., Huang, Y., Zhang, J., Chen, T., 2018. Giant gold nanowire vesicle-based colorimetric and SERS dual-mode immunosensor for ultrasensitive detection of *Vibrio parahemolyticus*. Anal. Chem. 90 (10), 6124–6130.
Guven, B., Dudak, F.C., Boyaci, I.H., Tamer, U., Ozsoz, M., 2014. SERS-based direct and sandwich assay methods for mir-21 detection. Analyst 139 (5), 1141–1147.
Hou, T., Li, W., Liu, X., Li, F., 2015. Label-free and enzyme-free homogeneous electrochemical biosensing strategy based on hybridization chain reaction: a facile, sensitive, and highly specific microRNA assay. Anal. Chem. 87 (22), 11368–11374.
Hu, X., Fan, J., Duan, B., Zhang, H., He, Y., Duan, P., Li, X., 2018. Single-molecule catalytic hairpin assembly for rapid and direct quantification of circulating miRNA biomarkers. Anal. Chim. Acta 1042, 109–115.
Huang, Y., Dai, L., Song, L., Zhang, L., Rong, Y., Zhang, J., Nie, Z., Chen, T., 2016. Engineering gold nanoparticles in compass shape with broadly tunable plasmon resonances and high-performance SERS. ACS Appl. Mater. Interfaces 8 (41), 27949–27955.
Huang, Y., Ferhan, A.R., Cho, S.J., Lee, H., Kim, D.H., 2015. Gold nanowire bundles grown radially outward from silicon micropillars. ACS Appl. Mater. Interfaces 7 (32), 17582–17586.
Jia, Y., Zhang, L., Song, L., Dai, L., Lu, X., Huang, Y., Zhang, J., Guo, Z., Chen, T., 2017. Giant vesicles with anchored tiny gold nanowires: fabrication and surface-enhanced Raman scattering. Langmuir 33 (46), 13376–13383.
Jou, A.F., Lu, C.H., Ou, Y.C., Wang, S.S., Hsu, S.L., Willner, I., Ho, J.A., 2015. Diagnosing the miR-141 prostate cancer biomarker using nucleic acid-functionalized CdSe/ZnS QDs and telomerase. Chem. Sci. 6 (1), 659–665.
Kim, J.W., Suh, K.D., 2008. Monodisperse polymer particles synthesized by seeded polymerization techniques. J. Ind. Eng. Chem. 14 (1), 1–9.
Lagos-Quintana, M., Rauhut, R., Lendeckel, W., Tuschl, T., 2001. Identification of novel genes coding for small expressed RNAs. Science 294 (5543), 853–858.
Lane, L.A., Qian, X., Nie, S., 2015. SERS nanoparticles in medicine: from label-free detection to spectroscopic tagging. Chem. Rev. 115 (19), 10489–10529.
Lee, S., Chon, H., Lee, J., Ko, J., Chung, B.H., Lim, D.W., Choo, J., 2014. Rapid and sensitive phenotypic marker detection on breast cancer cells using surface-enhanced Raman scattering (SERS) imaging. Biosens. Bioelectron. 51, 238–243.
Li, J., Skeete, Z., Shan, S., Yan, S., Kurzatkowska, K., Zhao, W., Ngo, Q.M., Holubovska, P., Luo, J., Hepel, M., Zhong, C.J., 2015a. Surface enhanced Raman scattering detection of cancer biomarkers with bifunctional nanocomposite probes. Anal. Chem. 87 (21), 10698–10702.
Li, S., Xu, L., Ma, W., Kuang, H., Wang, L., Xu, C., 2015b. Triple Raman label-encoded gold nanoparticle trimers for simultaneous heavy metal ion detection. Small 11 (28), 3435–3439.
Li, X., Ye, S., Luo, X., 2016. Sensitive SERS detection of miRNA via enzyme-free DNA machine signal amplification. Chem. Comm. 52 (67), 10269–10272.
Li, X., Zheng, F., Ren, R., 2015c. Detecting miRNA by producing RNA: a sensitive assay that combines rolling-circle DNA polymerization and rolling circle transcription. Chem. Comm. 51 (60), 11976–11979.
Li, Z., Lin, Z., Wu, X., Chen, H., Chai, Y., Yuan, R., 2017. Highly efficient electrochemiluminescence resonance energy transfer system in one nanostructure: its application for ultrasensitive detection of microRNA in cancer cells. Anal. Chem. 89 (11), 6029–6035.
Lin, S., Gregory, R.I., 2015. MicroRNA biogenesis pathways in cancer. Nat. Rev. Cancer 15 (6), 321–333.
Liu, M., Wang, Z., Zong, S., Chen, H., Zhu, D., Wu, L., Hu, G., Cui, Y., 2014. SERS detection and removal of mercury(II)/silver(I) using oligonucleotide-functionalized

core/shell magnetic silica sphere@Au nanoparticles. ACS Appl. Mater. Interfaces 6 (10), 7371–7379.
Liu, X.L., Liang, S., Nan, F., Yang, Z.J., Yu, X.F., Zhou, L., Hao, Z.H., Wang, Q.Q., 2013. Solution-dispersible Au nanocube dimers with greatly enhanced two-photon luminescence and SERS. Nanoscale 5 (12), 5368–5374.
Lu, J., Getz, G., Miska, E.A., Alvarez-Saavedra, E., Lamb, J., Peck, D., Sweet-Cordero, A., Ebert, B.L., Mak, R.H., Ferrando, A.A., Downing, J.R., Jacks, T., Horvitz, H.R., Golub, T.R., 2005. MicroRNA expression profiles classify human cancers. Nature 435 (7043), 834–838.
Lu, X., Huang, Y., Liu, B., Zhang, L., Song, L., Zhang, J., Zhang, A., Chen, T., 2018. Light-controlled shrinkage of large-area gold nanoparticle monolayer film for tunable SERS activity. Chem. Mater. 30 (6), 1989–1997.
Ma, D., Huang, C., Zheng, J., Tang, J., Li, J., Yang, J., Yang, R., 2018. Quantitative detection of exosomal microRNA extracted from human blood based on surface-enhanced Raman scattering. Biosens. Bioelectron. 101, 167–173.
Maruthappu, M., Watkins, J., Noor, A.M., Williams, C., Ali, R., Sullivan, R., Zeltner, T., Atun, R., 2016. Economic downturns, universal health coverage, and cancer mortality in high-income and middle-income countries, 1990–2010: a longitudinal analysis. Lancet 388 (10045), 684–695.
Nie, S., Emory, S.R., 1997. Probing single molecules and single nanoparticles by surface-enhanced Raman scattering. Science 275, 1102–1106.
Pang, Y., Wang, C., Wang, J., Sun, Z., Xiao, R., Wang, S., 2016. Fe_3O_4@Ag magnetic nanoparticles for microRNA capture and duplex-specific nuclease signal amplification based SERS detection in cancer cells. Biosens. Bioelectron. 79, 574–580.
Qian, Y., Fan, T., Yao, Y., Shi, X., Liao, X., Zhou, F., Gao, F., 2018. Label-free and Raman dyes-free surface-enhanced Raman spectroscopy for detection of DNA. Sens. Actuators B Chem. 254, 483–489.
Redshaw, N., Wilkes, T., Whale, A., Cowen, S., Huggett, J., Foy, C.A., 2013. A comparison of miRNA isolation and RT-qPCR technologies and their effects on quantification accuracy and repeatability. Biotechniques 54 (3), 155–164.
Robison, L.L., Hudson, M.M., 2014. Survivors of childhood and adolescent cancer: life-long risks and responsibilities. Nat. Rev. Cancer 14 (1), 61–70.
Rong, Y., Song, L., Si, P., Zhang, L., Lu, X., Zhang, J., Nie, Z., Huang, Y., Chen, T., 2017. Macroscopic assembly of gold nanorods into superstructures with controllable orientations by anisotropic affinity interaction. Langmuir 33 (48), 13867–13873.
Schwarzenbach, H., Hoon, D.S., Pantel, K., 2011. Cell-free nucleic acids as biomarkers in cancer patients. Nat. Rev. Cancer 11 (6), 426–437.
Stamplecoskie, K.G., Scaiano, J.C., Tiwari, V.S., Anis, H., 2011. Optimal size of silver nanoparticles for surface-enhanced Raman spectroscopy. J. Phys. Chem. C 115 (5), 1403–1409.
Su, J., Wang, D., Norbel, L., Shen, J., Zhao, Z., Dou, Y., Peng, T., Shi, J., Mathur, S., Fan, C., Song, S., 2017. Multicolor gold-silver nano-mushrooms as ready-to-use SERS Probes for ultrasensitive and multiplex DNA/miRNA detection. Anal. Chem. 89 (4), 2531–2538.
Thomson, J.M., Parker, J., Perou, C.M., Hammond, S.M., 2004. A custom microarray platform for analysis of microRNA gene expression. Nat. Methods 1 (1), 47–53.
Wang, Y., Yan, B., Chen, L., 2013. SERS tags: novel optical nanoprobes for bioanalysis. Chem. Rev. 113 (3), 1391–1428.
Wilson, A.J., Willets, K.A., 2014. Visualizing site-specific redox potentials on the surface of plasmonic nanoparticle aggregates with superlocalization SERS microscopy. Nano Lett. 14 (2), 939–945.
Wulfkuhle, J.D., Liotta, L.A., Petricoin, E.F., 2003. Proteomic applications for the early detection of cancer. Nat. Rev. Cancer 3 (4), 267–275.
Ye, L.P., Hu, J., Liang, L., Zhang, C.Y., 2014a. Surface-enhanced Raman spectroscopy for simultaneous sensitive detection of multiple microRNAs in lung cancer cells. Chem. Comm. 50 (80), 11883–11886.
Ye, S., Wu, Y., Zhang, W., Li, N., Tang, B., 2014b. A sensitive SERS assay for detecting proteins and nucleic acids using a triple-helix molecular switch for cascade signal amplification. Chem. Comm. 50 (66), 9409–9412.
Zeng, D., Ouyang, Q., Cai, Z., Xie, X.Q., Anderson, C.J., 2014. New cross-bridged cyclam derivative CB-TE1K1P, an improved bifunctional chelator for copper radionuclides. Chem. Comm. 50 (1), 43–45.
Zhang, C., You, E., Jin, Q., Yuan, Y., Xu, M., Ding, S., Yao, J., Tian, Z., 2017. Observing the dynamic "hot spots" on two-dimensional Au nanoparticles monolayer film. Chem. Commun. 53 (50), 6788–6791.
Zhang, H., Liu, Y., Gao, J., Zhen, J., 2015. A sensitive SERS detection of miRNA using a label-free multifunctional probe. Chem. Comm. 51 (94), 16836–16839.
Zhang, R., Zhang, Y., Dong, Z.C., Jiang, S., Zhang, C., Chen, L.G., Zhang, L., Liao, Y., Aizpurua, J., Luo, Y., Yang, J.L., Hou, J.G., 2013. Chemical mapping of a single molecule by plasmon-enhanced Raman scattering. Nature 498 (7452), 82–86.
Zheng, J., Ma, D., Shi, M., Bai, J., Li, Y., Yang, J., Yang, R., 2015. A new enzyme-free quadratic SERS signal amplification approach for circulating microRNA detection in human serum. Chem. Comm. 51 (90), 16271–16274.